

The Structure of Sodium Silicate Glass from Neutron Diffraction and Modelling of Oxygen-Oxygen Correlations

HANNON, Alex, VAISHNAV, Shuchi, ALDERMAN, Oliver and BINGHAM, Paul
<<http://orcid.org/0000-0001-6017-0798>>

Available from Sheffield Hallam University Research Archive (SHURA) at:

<https://shura.shu.ac.uk/28787/>

This document is the Published Version [VoR]

Citation:

HANNON, Alex, VAISHNAV, Shuchi, ALDERMAN, Oliver and BINGHAM, Paul (2021). The Structure of Sodium Silicate Glass from Neutron Diffraction and Modelling of Oxygen-Oxygen Correlations. *Journal of the American Ceramic Society*. [Article]

Copyright and re-use policy

See <http://shura.shu.ac.uk/information.html>

ORIGINAL ARTICLE

The structure of sodium silicate glass from neutron diffraction and modeling of oxygen-oxygen correlations

Alex C. Hannon¹  | Shuchi Vaishnav²  | Oliver L. G. Alderman¹  | Paul A. Bingham² ¹ISIS Facility, Rutherford Appleton Laboratory, Didcot, UK²Materials and Engineering Research Institute, College of Business, Technology and Engineering, Sheffield Hallam University, Sheffield, UK**Correspondence**Alex C. Hannon, ISIS Facility, Rutherford Appleton Laboratory, Chilton, Didcot, Oxon OX11 0QX, UK
Email: alex.hannon@stfc.ac.uk**Present address**

Shuchi Vaishnav, Department of Materials Science and Engineering, Sheffield, UK

Abstract

It is shown that modeling the first oxygen-oxygen peak in the neutron correlation function of a glass enables structural information about other correlations to be obtained, and the method is illustrated by application to a sodium silicate glass. The first O–O coordination number can be calculated from network theory, and sodium silicate crystal structures show that the mean O–O distance can be calculated from the Si–O distance, despite the distortion of the SiO₄ tetrahedra. Modeling the O–O peak for a sodium silicate glass allows the Na–O bond length distribution to be determined. For a binary glass with 42.5 mol% Na₂O, it is found that the Na–O coordination number is 4.8(2) with an average bond length of 2.45 Å, and the Na–O bond lengths are more widely distributed than in sodium silicate crystal structures. Sodium ions are bonded mostly to non-bridging oxygens (NBOs), and the Na–NBO coordination number may be four as in crystals. Sodium ions are also bonded to a smaller number of bridging oxygens (BOs). Contrary to previous reports, it is not concluded that Na–NBO bonds are shorter than Na–BO bonds, but instead that the Na–BO distribution is relatively narrow, whilst the Na–NBO distribution extends to both shorter and longer distance. The broad distribution of Na–O bond lengths arises from a relatively broad distribution of Na–NBO bond valences, subject to the overall requirement of charge balance.

KEYWORDS

bond length, glass, silicates, structure

1 | INTRODUCTION

Neutron diffraction is arguably the most reliable experimental method for the determination of the bond length distribution and coordination number of ions in glasses.¹ For a cation A in an oxide glass, this is achieved by analysis of the first A–O peak in the neutron correlation function. One of the main difficulties for this analysis can arise from the overlap between the

A–O peak and the first O–O peak, which arises from distances between pairs of oxygen atoms in the basic structural units. We show here that O–O coordination numbers can be calculated, even for complex glasses, provided that the environment of the glass network forming cations is known. The O–O coordination numbers can then be used as a basis for taking the O–O peak into account so that the bond length distribution of an ion can be revealed.

This is an open access article under the terms of the Creative Commons Attribution License, which permits use, distribution and reproduction in any medium, provided the original work is properly cited.

© 2021 The Authors. *Journal of the American Ceramic Society* published by Wiley Periodicals LLC on behalf of American Ceramic Society (ACERS)

Sodium silicate is the archetypal glass-forming system. For example, it is used in text books² to illustrate the structural roles of glass formers (SiO_2) and network modifiers (Na_2O). Alkali silicate glasses are of scientific interest for their ionic transport properties, and for example, it is a longstanding challenge to provide a fully satisfactory explanation of the mixed alkali effect in silicates and other glasses.^{3,4} However, despite the fundamental interest in sodium silicate glasses, a detailed understanding of the structural role of sodium in the silicate network is still lacking. For example, it is not well understood how sodium bonds to the bridging and non-bridging oxygens in the glass. There are surprisingly few reports of diffraction studies of sodium silicate glasses, and this may be due to the difficulties of interpretation that arise from the large overlap between the Na–O and O–O peaks in the correlation functions measured by diffraction; this difficulty is especially severe for neutron diffraction, for which the Na–O peak is relatively small. In this paper, we discuss in detail how the O–O peak in the neutron correlation function of a sodium silicate glass can be modeled to enable the distribution of Na–O bond lengths to be closely investigated.

2 | THEORETICAL OUTLINE

2.1 | Network theory

This paper is concerned in particular with the calculation of the O–O coordination numbers for various oxide networks. The coordination number n_{j-k} is the average number of k -type atoms at distance r_{j-k} (or at a small range of distances close to r_{j-k}) from a j -type atom. (The atom “type” j or k may indicate a specific element (Si, O, etcetera), or it may indicate a particular species of an atom, such as bridging or non-bridging oxygen.) For example, most phases of pure SiO_2 have a structure that, ideally, is a fully connected network of SiO_4 tetrahedra in which pairs of tetrahedra are connected together by the sharing of bridging oxygen (BO), as shown in Figure 1. All pairs of oxygen atoms within a tetrahedron are separated by almost exactly the same distance, $r_{(\text{O}-\text{O})\text{Si}}$, approximately 2.63 \AA .⁵⁻⁸ It is apparent from Figure 1 that for SiO_2 (for which all oxygens are BOs) the coordination number, $n_{(\text{O}-\text{O})\text{Si}}$, at this distance is six. The addition of a unit of modifier, such as Na_2O , to a silicate network results in the conversion of one BO to two non-bridging oxygens (NBOs), see Figure 2. The individual $(\text{O}-\text{O})_{\text{Si}}$ coordination number for each NBO site is three, and thus the addition of modifier leads to a reduction in the average coordination number, $n_{(\text{O}-\text{O})\text{Si}}$. The conversion of BOs to NBOs by the process shown in Figure 2 can be repeated until a composition $\sim 67 \text{ mol\% Na}_2\text{O}$, which is a theoretical limit for glass formation, assuming that the only types of oxygen are BO and NBO. In practice, it becomes very hard to form glass as this

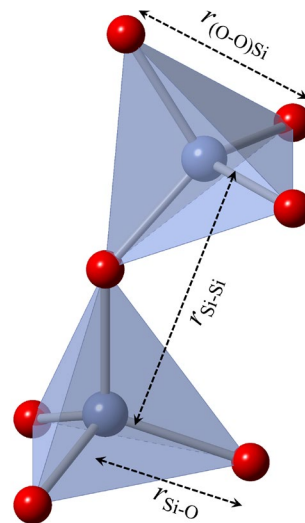


FIGURE 1 Connection of two corner-sharing SiO_4 tetrahedra by a bridging oxygen (larger blue spheres are silicon atoms; smaller red spheres are oxygen atoms). The oxygen-oxygen distance within a tetrahedron, $r_{(\text{O}-\text{O})\text{Si}}$, and the other two shortest distances are indicated

composition is approached, and the highest Na_2O content for which there are reliable reports of binary Na_2O - SiO_2 glass formation appears to be $64.29 \text{ mol\% Na}_2\text{O}$.^{9,10} Reports of glass formation with an apparent Na_2O content higher than this value are likely to arise as a consequence of carbonate retention.¹¹

More than one approach can be used to evaluate O–O coordination numbers for oxide networks, but the reasoning given here has the advantages that it is simple and provides a clear physical view: Let the number of atoms of type j in a sample be N_j , and consider distances between atoms of types j and k that have length in a certain range of interest; let there be N_{j-k} occurrences of j - k distances that are in the range of interest. The average j - k coordination number is then

$$n_{j-k} = \frac{N_{j-k} (1 + \delta_{jk})}{N_j}, \quad (1)$$

where the Kronecker delta, δ_{jk} , takes account of the fact that for like-atom ($j = k$) pairs both ends of the interatomic distance contribute to the coordination number of interest.

The number of $(\text{O}-\text{O})_{\text{Si}}$ distances within a single SiO_4 tetrahedron is six, and therefore for a silicate sample containing N_{Si} silicon atoms, the number of occurrences of the $(\text{O}-\text{O})_{\text{Si}}$ distance is $6N_{\text{Si}}$. Equation 1 then gives the $(\text{O}-\text{O})_{\text{Si}}$ coordination number as follows:

$$n_{(\text{O}-\text{O})\text{Si}} = \frac{12N_{\text{Si}}}{N_{\text{O}}}. \quad (2)$$

Thus, for a sodium silicate of composition $x\text{Na}_2\text{O} \cdot (1-x)\text{SiO}_2$, the $(\text{O}-\text{O})_{\text{Si}}$ coordination number is as follows:

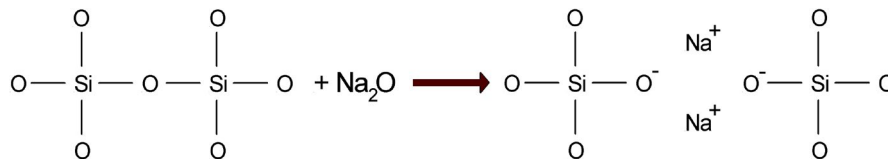


FIGURE 2 Addition of a unit of modifier, such as Na_2O , to a silicate network resulting in the conversion of one bridging oxygen to two non-bridging oxygens

$$n_{(\text{O}-\text{O})_{\text{Si}}} = \frac{12(1-x)}{2-x}. \quad (3)$$

As Na_2O is added to the glass, the number of $(\text{O}-\text{O})_{\text{Si}}$ distances in the SiO_4 tetrahedra remains unchanged (the numerator of Equation 2), but the number of oxygen atoms increases (the denominator of Equation 2), and hence the average $(\text{O}-\text{O})_{\text{Si}}$ coordination number declines, as shown in Figure 3A.

A binary silicate, such as sodium silicate, is a relatively simple system since there is only one glass former with only one basic structural unit (the SiO_4 tetrahedron), and hence the $(\text{O}-\text{O})_{\text{Si}}$ coordination number can be calculated without any other knowledge, as shown by the continuous line in Figure 3A. Nevertheless, Equation 1 can easily be applied to more complex systems. For example, consider a binary alkali borate such as $x\text{Li}_2\text{O} \cdot (1-x)\text{B}_2\text{O}_3$. Pure B_2O_3 glass is a fully connected network of corner-sharing BO_3 triangles,¹³ but the addition of a modifier such as Li_2O leads to a fraction N_4 of the boron-centred units becoming corner-sharing BO_4 tetrahedra,¹⁴ and also to the formation of NBOs, especially for higher Li_2O contents. The value of N_4 can be determined experimentally, and Figure 3B shows the values of N_4 for lithium borate glasses, measured over a very wide composition range by ^{11}B NMR.¹² In a borate glass, there are two different types of oxygen-oxygen distance, $(\text{O}-\text{O})_{\text{B}_3} \sim 2.36 \text{ \AA}$ within the BO_3 units, and $(\text{O}-\text{O})_{\text{B}_4} \sim 2.41 \text{ \AA}$ within the BO_4 units. Within a BO_3 unit, there are three oxygen-oxygen distances, while there are six oxygen-oxygen distances within a BO_4 unit. There are three different types of a bridge that may potentially occur in this system ($\text{BO}_3\text{-BO}_3$, $\text{BO}_3\text{-BO}_4$ and $\text{BO}_4\text{-BO}_4$), and for each of these, the individual BO has a different pair of O-O coordination numbers at the $(\text{O}-\text{O})_{\text{B}_3}$ and $(\text{O}-\text{O})_{\text{B}_4}$ distances, respectively. Furthermore, an individual NBO has a different O-O coordination number, depending on whether it is located on a BO_3 or BO_4 unit. As a consequence, it might perhaps be expected that it is not possible to predict the O-O coordination numbers for a mixed glass former without knowledge of whether there is a preference for, or avoidance of, $\text{BO}_3\text{-BO}_4$ bridges, and without knowledge of the preference of NBOs to be located on BO_3 or BO_4 units, but this is not the case. As the composition of a borate glass is changed, the respective numbers of $(\text{O}-\text{O})_{\text{B}_3}$ and $(\text{O}-\text{O})_{\text{B}_4}$ distances in each of

the units remain the same, regardless of the types of connection that form between the units. It then follows from Equation 1 that the two O-O coordination numbers are:

$$n_{(\text{O}-\text{O})_{\text{B}_3}} = \frac{6N_{\text{B}_3}}{N_{\text{O}}} = \frac{6N_{\text{B}}(1-N_4)}{N_{\text{O}}} = \frac{12(1-N_4)(1-x)}{3-2x}, \quad (4)$$

$$n_{(\text{O}-\text{O})_{\text{B}_4}} = \frac{12N_{\text{B}_4}}{N_{\text{O}}} = \frac{12N_{\text{B}}N_4}{N_{\text{O}}} = \frac{24N_4(1-x)}{3-2x}. \quad (5)$$

Figure 3A shows the variation of these two O-O coordination numbers with composition, together with the total O-O coordination number, $n_{(\text{O}-\text{O})_{\text{B}}} = n_{(\text{O}-\text{O})_{\text{B}_3}} + n_{(\text{O}-\text{O})_{\text{B}_4}}$. These coordination numbers can only be calculated at compositions for which N_4 is known, and hence they are shown as points in the figure, rather than a continuous line.

In either a trigonal or a tetrahedral structural unit (such as BO_3 and BO_4) the oxygen-oxygen distances are all very similar in length. Equation 1 can, however, also be applied to structural units in which the oxygen-oxygen distances are significantly different, provided that these distances are counted correctly. For example, a GeO_6 octahedron (which appears to occur in lanthanum borogermanate glass¹⁵) has 12 O-O distances corresponding to the octahedral edge length $\sqrt{2}r_{\text{Ge-O}}$, and three O-O distances corresponding to the octahedral axis $2r_{\text{Ge-O}}$.

2.2 | Neutron diffraction

Neutron diffraction (ND) is an important experimental technique that can be used to measure the coordination numbers of ions in glasses. The total neutron correlation function¹ is a weighted sum of partial correlation functions, $t_{l-l'}(r)$;

$$T(r) = \sum_{l,l'}^{l \geq l'} c_l (2 - \delta_{ll'}) \bar{b}_l \bar{b}_{l'} t_{l-l'}(r), \quad (6)$$

where the l and l' summations are over all unique pairs of atom types in the sample. c_l and \bar{b}_l are respectively the atomic fraction and coherent neutron scattering length for atom type l . A peak in the correlation function corresponds to a commonly occurring interatomic distance in the sample. An interatomic distance r_{j-k} , due to atom pair j and k , with

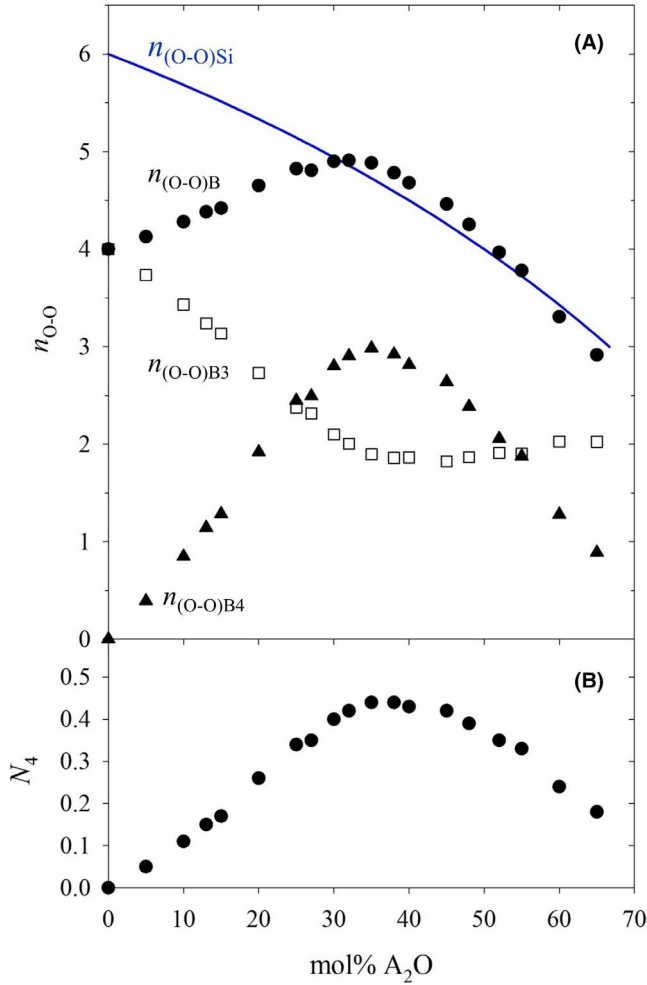


FIGURE 3 (A) Oxygen-oxygen coordination numbers: The O-O coordination number, $n_{(O-O)Si}$, (blue line) at the O-O distance in SiO_4 tetrahedra, as predicted by Equation 3 for Na_2O-SiO_2 glasses. The O-O coordination number, $n_{(O-O)B3}$, (open squares) at the O-O distance in BO_3 units, as predicted by Equation 4 and the experimental values of N_4 for $Li_2O-B_2O_3$ glasses. The O-O coordination number, $n_{(O-O)B4}$, (closed triangles) at the O-O distance in BO_4 units, as predicted by Equation 5 and the experimental values of N_4 for $Li_2O-B_2O_3$ glasses. The total predicted O-O coordination number, $n_{(O-O)B} = n_{(O-O)B3} + n_{(O-O)B4}$, (closed circles) for $Li_2O-B_2O_3$ glasses. (B) Experimental results for the fraction of boron atoms in $Li_2O-B_2O_3$ glasses that are four-coordinated, N_4 ¹²

coordination number n_{j-k} and RMS (root mean square) variation in distance $\langle u_{j-k}^2 \rangle^{\frac{1}{2}}$ contributes a peak to the relevant partial correlation function with the following form:

$$t_{j-k}(r) = \frac{n_{j-k}}{r_{j-k} \left(2\pi \langle u_{j-k}^2 \rangle \right)^{\frac{1}{2}}} \exp \left(-\frac{(r - r_{j-k})^2}{2 \langle u_{j-k}^2 \rangle} \right). \quad (7)$$

The coordination number is then related to the area, A_{j-k} , under the peak in $T(r)$, according to

$$A_{j-k} = \frac{n_{j-k} (2 - \delta_{ll'}) c_j \bar{b}_l \bar{b}_{l'}}{r_{j-k}}. \quad (8)$$

The $k-j$ and $j-k$ coordination numbers are not independent (provided that they are defined by the same interatomic distance), and it may be shown¹ that they are related by the identity

$$n_{k-j} = n_{j-k} \frac{c_j}{c_k}. \quad (9)$$

2.3 | Bond valence method

The bond valence (BV) method¹⁶⁻¹⁹ is an important empirical means to relate the coordination of atoms to their bond lengths, based on the determined structures of crystals. According to the BV method, the valence of the bond between two atoms, j and k , is considered to depend on the distance between them, d_{j-k} , and the most commonly used empirical formulation for this dependence²⁰ is given by

$$v_{j-k} = \exp \left(\frac{R_{j-k} - d_{j-k}}{b_{j-k}} \right), \quad (10)$$

where R_{j-k} is the BV parameter for the atom pair (j , k), determined from crystal structures, and b_{j-k} is the bond softness, originally treated as a universal constant ($=0.37 \text{ \AA}$),²¹ but more recently allowed to have different values depending on the atom pair.²² In this paper, the recent tabulation of revised BV parameters, R_{j-k} and b_{j-k} , reported by Gagné and Hawthorne²³ is used. An essential component of the method is Pauling's postulate,²⁴ which requires that the sum of the valences of the bonds to an atom should be equal (or nearly equal) to the formal valence of the atom

$$V_j = \sum_k v_{j-k}. \quad (11)$$

This is essentially a more sophisticated expression of the need for charge balance.

The distortion theorem¹⁸⁻²⁸ is an important consequence of the bond valence model, and it may be stated as follows: any deviation of a bond length from the average bond length causes the average bond length to increase. For example, consider a SiO_4 tetrahedron. If all four Si-O bonds have a valence of one, then according to Equation 10, their length (and the average length too) is R_{SiO} . If one of the bonds is shortened to $R_{SiO} - \Delta d$, its valence is increased to $1 + \Delta v$. According to Equation 11, a decrease in the valence of Δv must be distributed among the other three Si-O bonds. This deficit may, for example,

be assigned to only one of these three bonds so that it has a valence of $1-\Delta v$. Due to the exponential form of Equation 10, this decrease in valence leads to the length of the bond increasing by more than Δd . Thus, if the lengths of the four Si-O bonds become unequal, then this leads to an increase in the average of their lengths.

For a crystal structure, each atomic site has a finite number of bond lengths, d_{j-k} , and the valence sum for the bonds to the site can be determined by calculating the valence for each of the bonds according to Equation 10. In contrast, for a glass, discrete values of the lengths of the bonds to a site are not experimentally available. It is thus useful¹⁶ to define a generalized valence sum function, according to

$$V_j(r) = \int_0^r n_{j-k}(r') \exp\left(\frac{R_{j-k} - r'}{b_{j-k}}\right) dr'. \quad (12)$$

Here $n_{j-k}(r) = r t_{j-k}(r)$ is the partial radial distribution function, defined so that $n_{j-k}(r)dr$ is the average number of atoms of type k that are found in a spherical shell of radii $(r, r+dr)$ centred on an origin atom of type j . $V_j(r)$ represents the contribution to the valence sum of the average atom of type j due to all $j-k$ bonds shorter than r .

3 | THE STRUCTURE OF SODIUM SILICATE GLASS

3.1 | Neutron diffraction peak analysis

Figure 4 shows the neutron correlation function, $T(r)$, for a sodium silicate glass with 42.50 mol% Na₂O.²⁹ The ND measurement was made as part of a wider ranging study of the incorporation of sulphate in silicate glasses, and full experimental details are given in the previous publication.²⁹ The GEM diffractometer³⁰ was used to measure the diffraction pattern, which was Fourier transformed using the Lorch modification function¹ with a maximum momentum transfer, Q_{\max} , of 43 \AA^{-1} , to yield a correlation function with a high real-space resolution, as shown in the Figure 4. The first peak in $T(r)$ at about 1.62 \AA is due to Si-O bonds, while the second pronounced peak at about 2.65 \AA is due to $(\text{O}-\text{O})_{\text{Si}}$ distances in SiO₄ units (see Figure 1). On the assumption of a single value for the bond length, a very close fit to the first Si-O peak was obtained using *pf* software,³¹ and the fit parameters are given in Table 1. There is a large shoulder on the short distance side of the $(\text{O}-\text{O})_{\text{Si}}$ peak due to Na-O bonds, and the distribution of Na-O bond lengths is of interest but is not straightforward to determine. The method described here for determining the Na-O distribution essentially involves the subtraction

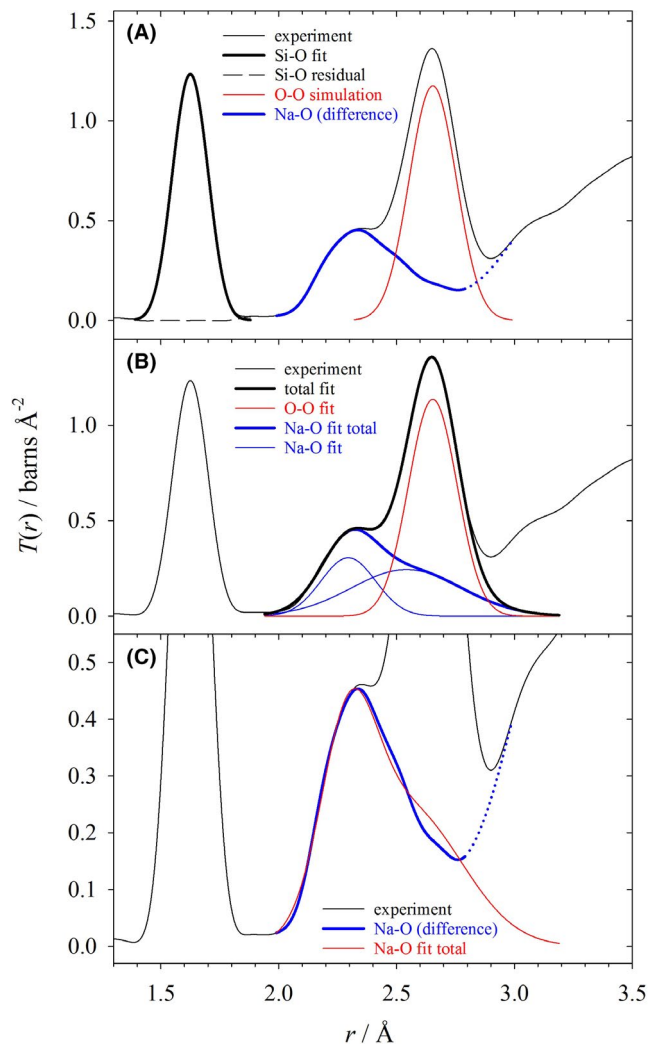


FIGURE 4 Estimation of the Na-O distribution from the neutron correlation function (thin black line) for sodium silicate glass with 42.5 mol% Na₂O. (A) A fit to the Si-O peak (thick black line) and its residual (dashed line). Also shown is a simulation of the peak arising from $(\text{O}-\text{O})_{\text{Si}}$ distances (thin red line), and the difference from subtraction of this simulation (thick blue line), which provides an estimate of the Na-O distribution. (B) A fit of one $(\text{O}-\text{O})_{\text{Si}}$ peak (thin red line) and two Na-O peaks (thin blue lines) to the 2.06 \AA – 2.80 \AA region. The thick blue line shows the total fitted Na-O contribution. (C) Comparison of the difference (thick blue line) and fit (thin red line) estimations of the Na-O contribution.

of a detailed prediction of the $(\text{O}-\text{O})_{\text{Si}}$ peak. Three parameters are required to predict the $(\text{O}-\text{O})_{\text{Si}}$ peak, namely its position, coordination number, and width, and these parameters are discussed in detail below.

The fitted mean Si-O bond length is longer than in pure SiO₂ glass but is consistent with the values for sodium silicate crystal structures, which show a general lengthening as the sodium content is increased (see Table 2, which gives a survey of the structural parameters of

	$j-k$	$r_{j-k} / \text{\AA}$	$\langle u_{j-k}^2 \rangle^{1/2} / \text{\AA}$	n_{j-k}	n_{k-j}
Si-O peak fit	Si-O	1.6249 (2)	0.0584 (3)	4.01 (1)	1.465 (3)
(O-O) _{Si} peak simulation	O-O	2.6535	0.089	4.381	
Three peak fit	O-O	2.6535 ^a	0.0929 (4)	4.381 ^a	
	Na-O	2.295 (2)	0.107 (3)	1.7 (1)	0.93 (6)
	Na-O	2.54 (1)	0.229 (6)	3.1 (1)	1.66 (7)
	ΣNa-O			4.8 (2)	2.59 (9)

Statistical errors from the fits are given in parentheses.

^aFixed.

sodium silicate crystals, and Figure 5A). Si-NBO bonds are shorter than Si-BO bonds; for example, in the reported structure of crystalline Na₂SiO₃,³² the difference between these two bond lengths is 0.080 Å. However, the observed Si-O peak in $T(r)$ is too broad to resolve this difference due to the combined effects of both thermal atomic motion and real-space resolution (which has a full width at half maximum of 0.126 Å for the Lorch modification function¹ with $Q_{\text{max}} = 43 \text{ \AA}^{-1}$). Nevertheless, the distortion theorem (see Section 2.3) shows that the lengthening of the mean Si-O bond length is evidence of the increasing variation in Si-O bond lengths, consistent with the presence of BOs and NBOs.

The fitted Si-O coordination number is close to four (Table 1), and it is assumed that essentially all silicon atoms are at the center of SiO₄ tetrahedra (Figure 1). For an undistorted SiO₄ tetrahedron (in which the Si is at the center of a tetrahedron of equally separated oxygens), the (O-O)_{Si} distance is $\sqrt{8/3} r_{\text{Si-O}} \approx 2.6535 \text{ \AA}$. Nevertheless, the tetrahedra in most materials are distorted, and Table 2 presents values for a tetrahedral distortion parameter, defined as follows:

$$\eta_{\text{tet}} = \frac{\langle r_{\text{Si-O}} \rangle}{\langle r_{(\text{O-O})_{\text{Si}}} \rangle} \sqrt{\frac{8}{3}}, \quad (13)$$

where $\langle r_{\text{Si-O}} \rangle$ and $\langle r_{(\text{O-O})_{\text{Si}}} \rangle$ are the mean Si-O bond length and the mean O-O distance along a tetrahedral edge. The values of the mean (*i.e.*, averaged over all crystallographic sites) tetrahedral distortion parameter for sodium silicate crystals and glasses (see Table 2 and Figure 5C) differ little from one, and thus the SiO₄ tetrahedra in sodium silicates are distorted in such a way that the ratio of the two mean distances is very close to the value for an undistorted tetrahedron. In comparison, the distortion of the PO₄ tetrahedra in phosphates (*i.e.*, $\langle \eta_{\text{tet}} \rangle - 1$) is an order of magnitude larger. For example, for crystalline NaPO₃,⁴¹ the parameter has a value $\langle \eta_{\text{tet}} \rangle = 1.0033$. (Note that the parameter η_{tet} is defined to be directly applicable to the analysis of glass diffraction data, which are sensitive to mean interatomic distances, but η_{tet} is not an exact measure of the distortion of the tetrahedra. It is

TABLE 1 Peak parameters for the neutron correlation function of a sodium silicate glass with 42.5 mol% Na₂O. (r_{j-k} is the interatomic distance between atoms j and k , while $\langle u_{j-k}^2 \rangle^{1/2}$ is the root mean square variation in r_{j-k} , and n_{j-k} is the coordination number.)

possible for a tetrahedron to be distorted in terms of the individual distances such that η_{tet} is exactly one, but such distortion is not directly relevant to the method used here for the simulation of the (O-O)_{Si} peak. More exact measures of tetrahedral distortion are known,⁴² but they require full knowledge of the three-dimensional geometry of the tetrahedra, and hence are not directly applicable to the interpretation of glass diffraction results.) The small deviations of η from one for sodium silicates show that to a good approximation the mean (O-O)_{Si} distance can be calculated from the mean Si-O distance without taking tetrahedral distortion into account, and the (O-O)_{Si} peak in $T(r)$ was modelled using the distance calculated for an undistorted SiO₄ tetrahedron with the measured mean Si-O bond length. For the composition of this glass, Equation 3 shows that the (O-O)_{Si} coordination number is 4.381. The root mean square (RMS) variation in (O-O)_{Si} distance, $\langle u_{(\text{O-O})_{\text{Si}}}^2 \rangle^{1/2}$, has been measured for pure SiO₂ glass⁶ as 0.089 Å, and this value was used, together with the calculated (O-O)_{Si} distance and coordination number, to calculate the simulation of the (O-O)_{Si} peak shown in Figure 4A (thin red line). The (O-O)_{Si} simulation was subtracted from the total correlation function to yield an initial estimate of the Na-O distribution (thick blue line). For distances longer than about 2.8 Å there may be contributions from other atom pairs (Si-Si, second Si-O, Na-Na, and Si-Na), and hence the difference is shown dotted in this region. The distribution of Na-O bond lengths is clearly asymmetric, with a narrower leading edge, a peak at 2.34 Å, and a broader trailing edge.

To further characterize the Na-O distribution, three peaks ((O-O)_{Si} and two Na-O) were fitted to $T(r)$ over a range below 2.80 Å, avoiding influence from other longer interatomic distances (the upper limit of the fitting range is similar to the length of the longest Na-O bonds, $r_{\text{Na-O,max}}$, as given in Table 2). The position and area of the (O-O)_{Si} peak were fixed at the calculated values, but its width was allowed to vary. The parameters for this fit are given in Table 1, and the fitted width of the (O-O)_{Si} peak, 0.0929(4) Å, is larger than the value for pure SiO₂ glass, 0.089 Å,⁶ which may be explained as follows: First, note that the width of a peak in $T(r)$ arises from

TABLE 2 Structural parameters of sodium silicate crystal structures and glasses. $\langle r_{\text{Si-O}} \rangle$ and $\langle r_{\text{O-Si}} \rangle$ are respectively the mean Si-O bond length and the mean (O-O)_{Si} distance, and $\langle \eta_{\text{tet}} \rangle$ is the mean tetrahedral distortion parameter (see Equation 13). $r_{\text{Na-O,max}}$ is the longest Na-O bond length, and the n_{i-k} values are the various coordination numbers for sodium-oxygen interactions. Only the α and β phases of Na₂Si₂O₅ are included, because crystallisation of glass shows that only these two polymorphs have any true range of thermodynamic stability³³

Compound	mol% Na ₂ O	$\langle r_{\text{Si-O}} \rangle / \text{\AA}$	$\langle r_{\text{O-Si}} \rangle / \text{\AA}$	$\langle \eta_{\text{tet}} \rangle$	$r_{\text{Na-O,max}} / \text{\AA}$	$n_{\text{Na-NBO}}$	$n_{\text{Na-BO}}$	$n_{\text{Na-O}}$	$n_{\text{NBO-Na}}$	$n_{\text{BO-Na}}$	$N_{\text{-Na}}$
SiO ₂ glass ⁸	0	1.608(4)	2.626(6)	0.99994							
α -SiO ₂ ³⁴	0	1.6088	2.6271	1.00001							
Na ₂ Si ₃ O ₇ ³⁵	25	1.6252	2.6511	1.00108	2.875	2.5	2.5	5	2.5	1	1.43
Na ₆ Si ₈ O ₁₉ ³⁶	27.27	1.6158	2.6400	0.99946	2.729	4	1.33	5.33	4	0.62	1.68
α -Na ₂ Si ₂ O ₅ ³⁷	33.33	1.6169	2.6409	0.99981	2.600	4	1	5	4	0.67	2
β -Na ₂ Si ₂ O ₅ ³⁸	33.33	1.6243	2.6545	0.99922	2.588	4	1.5	5.5	4	1	2.2
42.5Na ₂ O·57.5SiO ₂ glass, this work	42.50	1.62491 (6)						4.8 (2)			2.59 (9)
Na ₂ SiO ₃ ³²	50	1.6323	2.6653	1.00007	2.549	4	1	5	4	2	3.33
Na ₆ Si ₂ O ₇ ³⁹	60	1.6285	2.6594	0.99999	2.869	4.33	0.33	4.67	4.33	2	4
Na ₄ SiO ₄ ⁴⁰	66.67	1.6436	2.6830	1.00033	2.482	4.5	0	4.5	4.5		4.5

The structural parameters of all known phases of Na₂Si₂O₅ are given in Table S3.

both thermal and static disorder.¹ Second, ²⁹Si MAS (magic angle spinning) NMR measurements on sodium silicate glasses^{43,44} consistently show that a glass with 42.5 mol% Na₂O is dominated by approximately equal numbers of Q₃ and Q₂ species (Q_n indicates a SiO₄ tetrahedron in which the numbers of BOs and NBOs are n and $4-n$, respectively). In a Q₃ species there are both BO-BO and NBO-BO distances, whilst a Q₂ species additionally has NBO-NBO distances. In contrast, a Q₄ species in pure SiO₂ has only BO-BO distances, and thus it is to be expected that the sodium silicate glass has more (O-O)_{Si} static disorder than occurs for pure SiO₂, leading to a broader (O-O)_{Si} peak. The fitted Na-O peaks shown in Figure 4B are thus derived from a reasonable estimate of the form of the (O-O)_{Si} peak, and have the advantage of giving an estimate of the Na-O distribution that extends to longer distance in a reasonable way. Nevertheless, it is not likely that the Na-O distribution is formed of two discrete peaks, and it is more likely that it is a smooth, continuous distribution. The comparison of the initial and final estimates of the Na-O distribution in Figure 4C shows that the exact form of the longer distance part of the distribution is sensitive to the value for the width of the (O-O)_{Si} distribution. The numerical data for this estimate of the Na-O distribution are available from the ISIS Disordered Materials Database.⁴⁵

3.2 | Coordination numbers and related crystal structures

It is useful to compare the total Na-O and O-Na coordination numbers from the fit to the glass correlation function (Table 1) with the sodium-oxygen coordination numbers in (ambient pressure) sodium silicate crystal structures. (High pressure crystal phases are not considered, because these can have octahedral silicon sites, which profoundly alters the types of oxygen sites, see Section 3.4 below.) Bridging and non-bridging oxygens in a crystal structure can be differentiated unambiguously, and Table 2 gives both the total sodium-oxygen coordination numbers ($n_{\text{Na-O}}$ and $n_{\text{O-Na}}$) and the sodium-oxygen coordination numbers for each of these types of oxygen alone. Note that the Na-NBO and NBO-Na coordination numbers are equal: As shown in Figure 2, the addition of one unit of Na₂O to a silicate glass leads to the formation of two NBOs, so that there are equal numbers of Na and NBO in the glass, and hence the identity of Equation 9 shows that these two coordination numbers must be equal. As will be shown below, the equality of these two coordination numbers is a useful property for gaining an understanding of the structure; insight into the Na-NBO coordination can be gained by consideration of the the

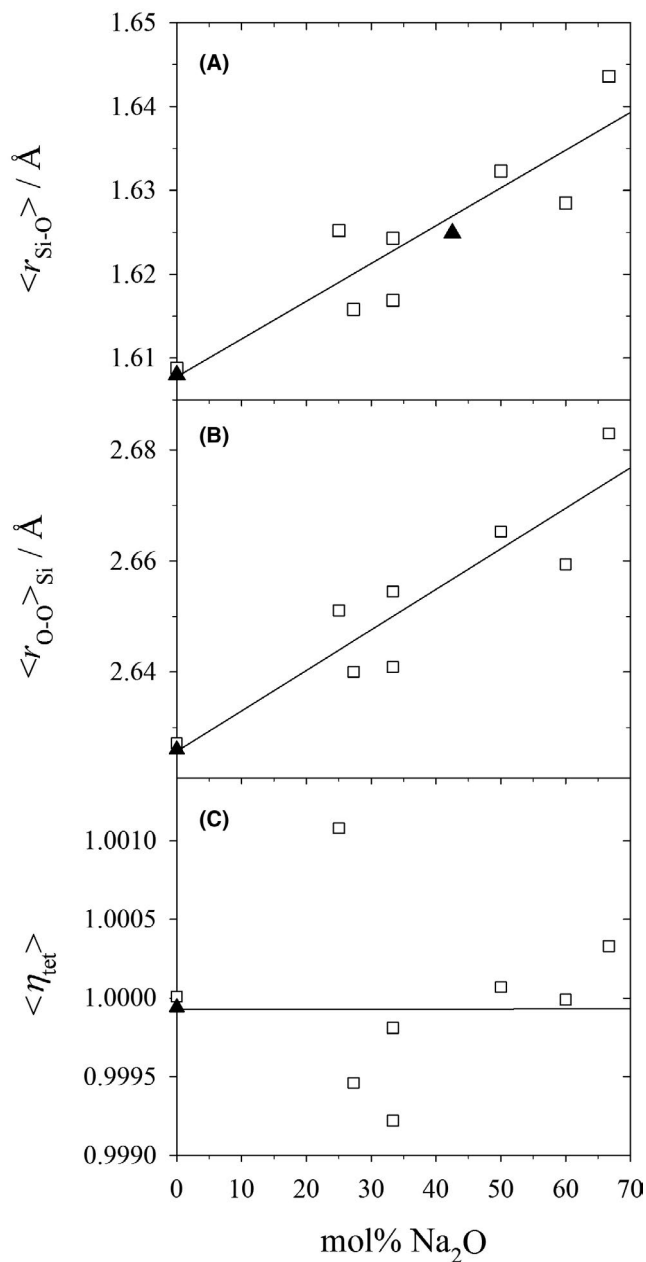


FIGURE 5 Mean Si–O bond length (A), $\langle r_{\text{Si-O}} \rangle$, mean (O–O)_{Si} distance (B), $\langle r_{\text{O-O}} \rangle_{\text{Si}}$, and mean tetrahedral distortion parameter (C), $\langle \eta_{\text{tet}} \rangle$, in ambient pressure sodium silicate crystal structures (open squares) and glasses (closed black triangles)

NBO–Na coordination. The sodium–oxygen coordination numbers for sodium silicate crystal structures are also plotted in Figure 6, and in the intermediate composition range 27.27–50 mol% Na₂O, the Na–NBO, and NBO–Na coordination numbers are constant at a value of four (this is true for each of the individual atomic sites in the crystal structures, as well as for the average over all sites). There is clearly a preference for these two coordination numbers to be four. Apart from this region of constancy for the Na–NBO and NBO–Na coordination numbers, the trends with composition are as might be expected:

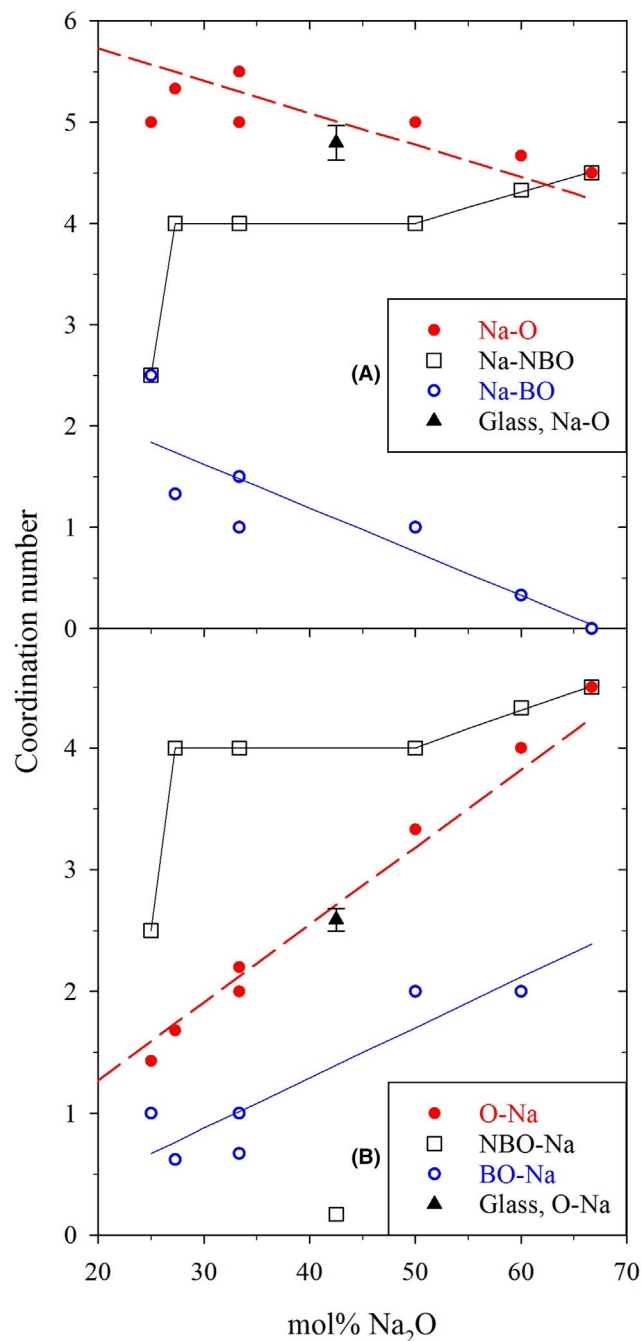


FIGURE 6 Average coordination numbers for ambient pressure sodium silicate crystal structures. (A) Sodium–oxygen coordination numbers: Na–O (closed red circles), Na–NBO (open black squares), Na–BO (open blue circles), and glass (Na–O, closed black triangle with error bar). (B) Oxygen–sodium coordination numbers: O–Na (closed red circles), NBO–Na (open black squares), BO–Na (open blue circles), and glass (O–Na, closed black triangle with error bar). The continuous lines are guides to the eye, whilst the dashed line is a fit in which $n_{\text{O-Na}}$ is proportional to the Na₂O content

As Na₂O is added to the silicate, there is a growth in the number of sodium atoms, and there is a corresponding increase in all three oxygen–sodium coordination

numbers (O–Na, NBO–Na and BO–Na, see Figure 6B). As Na₂O is added to the silicate, there is a growth in the number of NBOs with a corresponding growth in the Na–NBO coordination number, and there is a decline in the number of BOs with a corresponding decline in the Na–BO coordination number (see Figure 6A). It is striking to note that the total O–Na coordination number for the crystal structures (closed red circles in Figure 6A) is almost exactly proportional to the molar fraction of Na₂O, and a simple fit leads to an empirical model for this coordination number

$$n_{\text{O–Na}} = 6.37x, \quad (14)$$

and Equation 9 shows that this is equivalent to

$$n_{\text{Na–O}} = 6.37 - 3.18x. \quad (15)$$

These relations are shown by dashed red lines in Figure 6, and the coordination numbers for the glass (filled black triangles) are consistent with them, and with the trends for the crystal coordination numbers. The total Na–O coordination number for the glass, $n_{\text{Na–O}} = n_{\text{Na–NBO}} + n_{\text{Na–BO}} = 4.8(2)$, at an average Na–O bond length 2.45 Å, is significantly larger than the value of four which is found for the Na–NBO coordination number for all Na sites in ambient pressure crystal phases in the intermediate composition range. It is thus very likely that sodium ions in the glass are bonded to BOs, as well as NBOs, as is the case for sodium ions in the crystals. Nevertheless, note that the sodium–oxygen coordination is dominated by Na–NBO, with a relatively small contribution due to Na–BO.

3.3 | Na–O bond length distribution

The simple diagram shown in Figure 2 for the formation of NBOs gives the impression that Na⁺ ions bond only to NBOs, but this is too simplistic and it has long been realised that Na⁺ ions also bond to BOs in glasses. For example, in the schematic representation of a sodium silicate glass network shown by Warren and Bischof in 1936⁴⁶ on the basis of X-ray diffraction analysis, Na⁺ ions are shown with BOs in their coordination shell, as well as NBOs. Nevertheless, as pointed out by Nesbitt et al.,⁴⁷ there was no direct experimental verification of the presence of Na–BO bonds in glass until their X-ray Photoelectron Spectroscopy (XPS) study in 2015. Prior to that date, the main support for the presence of Na–BO bonds was that they are found in sodium silicate crystal structures (see Table 2), further supported by the results of molecular dynamics (MD) simulations.^{48,49} Although a relatively large number of MD simulations have been reported for sodium

silicate glasses,^{49–64} information about the sodium coordination is rarely reported in detail. The only detailed MD report for compositions close to 42.5 mol% Na₂O is given by Du and Cormack,⁴⁸ who predict that a sodium silicate glass with 40 mol% Na₂O has a mean Na–O bond length of 2.392 Å and a total Na–O coordination number of about 5.1, of which 3.9 is due to Na–NBO bonds, and 1.2 is due to Na–BO bonds. This predicted Na–NBO coordination number is similar to the value of four for crystals of intermediate composition (see Table 2 and Figure 6). On the other hand, Du and Cormack predict that in glasses the total Na–O coordination number increases as the Na₂O content increases, whereas crystal structures show a decline (see Equation 15). The increase predicted by MD appears to be inconsistent with the frequency of the far infrared Na vibration band at ~200 cm⁻¹,⁶⁵ which increases as Na₂O is

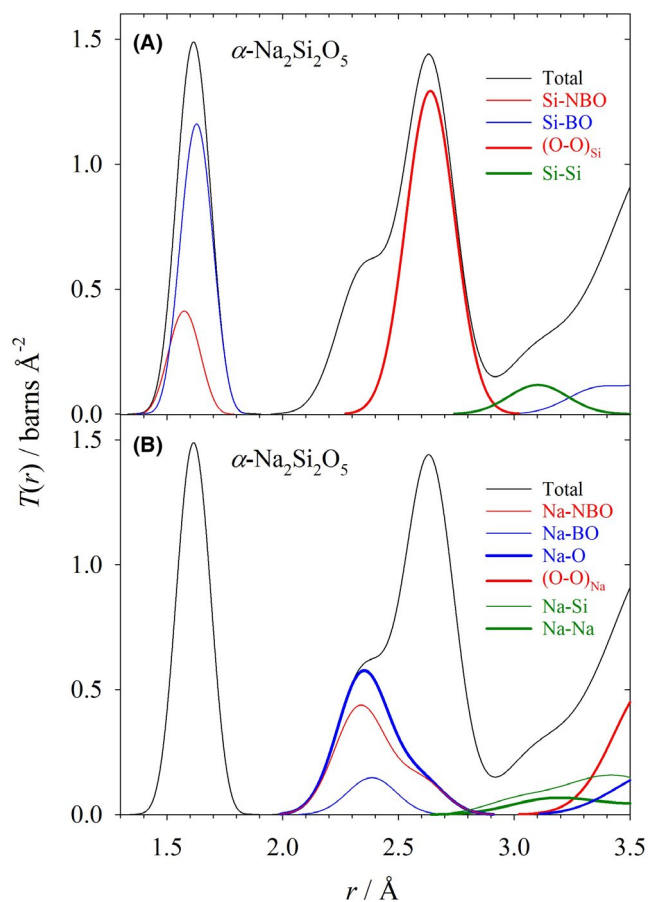


FIGURE 7 Simulation of the total neutron correlation function, $T(r)$, for crystalline $\alpha\text{-Na}_2\text{Si}_2\text{O}_5$ ³⁷ (thin black line). (A) Showing the silicate partial contributions as follows: Si–NBO (thin red line), Si–BO (thin blue line), (O–O)_{Si} (thick red line), and Si–Si (thick green line). (B) Showing the soda partial contributions as follows: Na–NBO (thin red line), Na–BO (thin blue line), total Na–O (thick blue line), (O–O)_{Na} (thick red line), Na–Si (thin green line), and Na–Na (thick green line)

added to SiO_2 ; this increase is evidence for a strengthening of the average Na-O bond, which corresponds to a progressive reduction of the average coordination number.

It is clear that the distribution of Na-O bond lengths in the glass (see Figure 4) has a sharper leading edge that is well determined, and a broader trailing edge with somewhat greater uncertainty for the exact form of the trailing edge. Sodium silicate crystals have a similar asymmetric distribution of Na-O bond lengths. Figure 7 shows a simulation of the total neutron correlation function for the reported crystal structure of $\alpha\text{-Na}_2\text{Si}_2\text{O}_5$ ³⁷ (~33.3 mol% Na_2O), together with its constituent partial contributions, with the BOs and NBOs treated as different atomic species. The simulated correlation functions were calculated using XTAL software,^{66,67} and are broadened for the same real-space resolution as the measured glass correlation function, and are also broadened for thermal motion using the widths given in Table S1. (See also Figure S5, which shows simulated correlation functions for crystalline $\beta\text{-Na}_2\text{Si}_2\text{O}_5$ ³⁸ and Na_2SiO_3 .³²) Of most importance to this discussion is the thermal width, 0.095 Å, for Na-O bonds, which was determined from a ND measurement (see Supporting Information) on crystalline Na_2SiO_3 .³² It is apparent from Figure 7 that the Si-NBO bonds are shorter than the Si-BO bonds in $\alpha\text{-Na}_2\text{Si}_2\text{O}_5$, which may be interpreted as arising from the NBOs being more negatively charged than the BOs. In previous ND studies of sodium silicate glass, Clare et al.⁶⁸ and then Wilding et al.⁶⁹ have proposed that in a similar way the shorter Na-O distances arise from NBOs, while the longer Na-O distances arise from BOs. However, it is clear from Figure 7 that this is not the case for crystalline $\alpha\text{-Na}_2\text{Si}_2\text{O}_5$. Instead, the Na-BO bonds in this crystal have a single length, 2.404 Å, whereas the Na-NBO bonds are broadly distributed, so that some are shorter and some are longer than the Na-BO bonds. In fact, similar distributions of Na-BO and Na-NBO bond lengths occur in other sodium silicate crystal structures. Figure 8 shows comparisons of the fit-derived Na-O partial correlation function for the glass, $t_{\text{Na-O}}(r)$ (see Equation 6), with simulations of the Na-O, Na-BO, and Na-NBO partial correlation functions for three crystal structures with similar compositions to the glass, $\alpha\text{-Na}_2\text{Si}_2\text{O}_5$,³⁷ $\beta\text{-Na}_2\text{Si}_2\text{O}_5$,³⁸ and Na_2SiO_3 .³² The Na-O partial correlation function for the glass is broader than $t_{\text{Na-O}}(r)$ for each of these crystal structures, extending a little further towards shorter distances, and extending more towards longer distances. Furthermore, all of these crystal structures have a narrow distribution of Na-BO bonds, and a distribution of Na-NBO bonds that is broader and extends to both shorter and longer distances than the Na-BO bonds. It is therefore very likely that the distributions of Na-BO and Na-NBO bond lengths in the glass are similar. Rather than the short Na-NBO and long Na-BO bonds proposed by Clare et al.,⁶⁸ it is much more likely

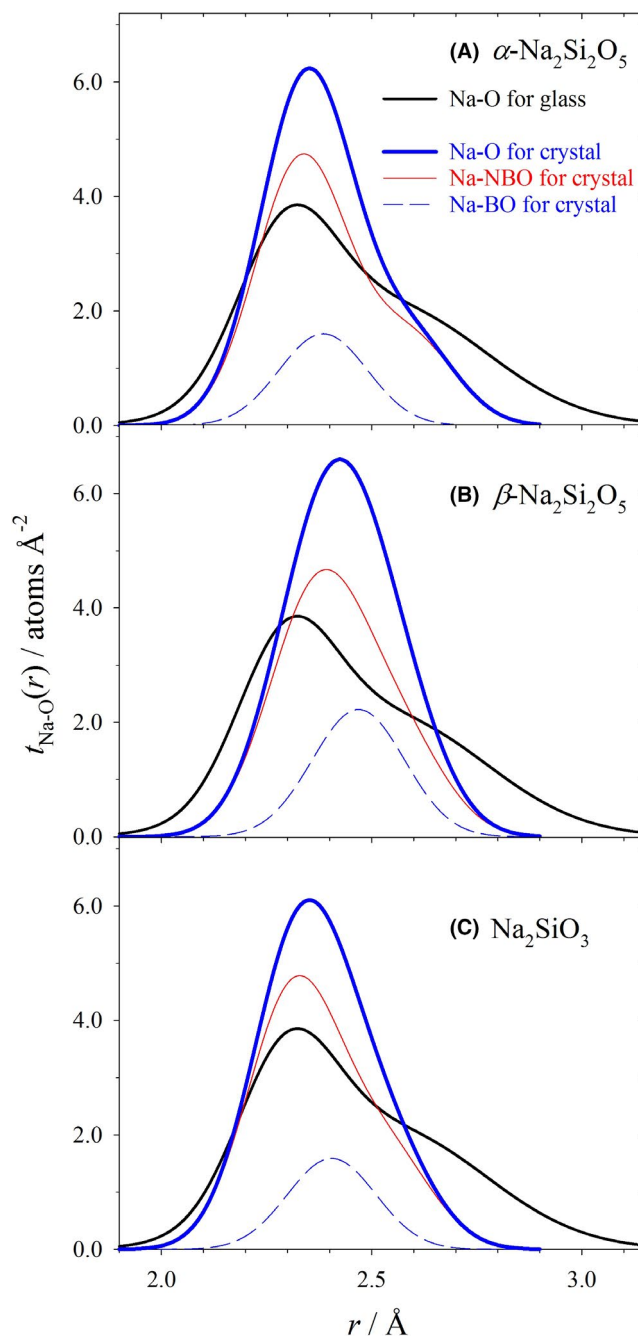


FIGURE 8 Na-O partial correlation functions, $t_{\text{Na-O}}(r)$, in sodium silicates. The total fitted Na-O partial correlation function in the glass with 42.5 mol% Na_2O (thick black line) is compared with the simulated Na-O function (thick blue line) for reported structures of sodium silicate crystals with similar composition: (A) $\alpha\text{-Na}_2\text{Si}_2\text{O}_5$,³⁷ (B) $\beta\text{-Na}_2\text{Si}_2\text{O}_5$,³⁸ and (C) Na_2SiO_3 .³² Also shown for the crystal structures are the Na-NBO and Na-BO functions (thin red and dashed blue lines respectively)

that the Na-BO bonds in the glass have a narrow distribution, whilst the distribution of Na-NBO bonds in the glass is broader, extending to both shorter and longer distances than the Na-BO bonds. An analysis using the bond valence method provides insight into how these distributions arise.

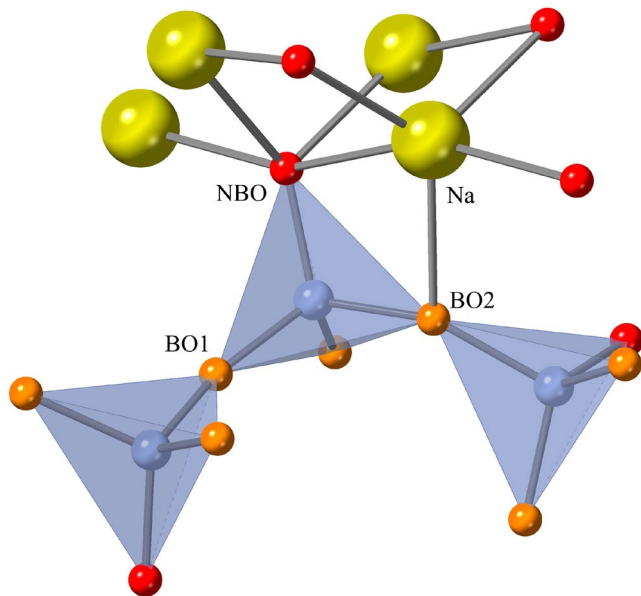


FIGURE 9 Local structure in crystalline α - $\text{Na}_2\text{Si}_2\text{O}_5$.³⁷ Silicon atoms (blue spheres) are shown at the centre of a tetrahedron of oxygen atoms. Bridging oxygen (BO) atoms are shown as orange spheres, and non-bridging oxygen (NBO) atoms are shown as red spheres. Large yellow spheres represent sodium atoms. Labelled atoms (and all silicons) are shown with their full complement of neighbors

3.4 | Local structure and bond valence analysis

Figure 9 shows the local structure in crystalline α - $\text{Na}_2\text{Si}_2\text{O}_5$.³⁷ The silicate network is formed of Q_3 units, with one NBO in each SiO_4 tetrahedron, and the NBO site is bonded to four Na^+ ions. The Na^+ site is bonded to five oxygens; it is necessarily bonded to four NBOs, and also to one BO. The NaO_5 polyhedron can be described as a distorted trigonal bipyramid,³⁷ and the $(\text{O}-\text{O})_{\text{Na}}$ edge distances in this unit (excluding one edge that is shared with the adjacent SiO_4 tetrahedron) have a broad distribution centred at 3.635 Å. Thus $(\text{O}-\text{O})_{\text{Na}}$ distances are too long to have any influence on the analysis presented in this paper. There are two BO sites, one of which is a ‘pure’ bridging oxygen, bonded only to two Si atoms, whilst the other is also bonded to one Na^+ ion. These structural features are typical of sodium silicate crystal structures, as summarized in Table 2. A BV analysis of the bond lengths in crystalline α - $\text{Na}_2\text{Si}_2\text{O}_5$ ³⁷ is given in Table 3; this analysis illustrates the behavior of valence sums that underlies the discussion of glass structure that follows. In this table, the lengths of the bonds to each site have been calculated from the reported crystal structure by the *XTAL* program,^{66,67} and then the

TABLE 3 Bond lengths in crystalline α - $\text{Na}_2\text{Si}_2\text{O}_5$,³⁷ together with an analysis of bond valences, calculated using the revised BV parameters reported by Gagné and Hawthorne²³

Origin site, <i>j</i>	Site multiplicity	Coordination number, ^a n_{j-M}	Motif	Coordinating site, <i>k</i>	Bond length, $d_{j-k}/\text{Å}$	Bond valence, v_{j-k}/e	Sum of valences/ <i>e</i>
Si1	8	4	SiO_4	NBO	1.578	1.125	4.083
				BO1	1.609	1.040	
				BO2	1.638	0.965	
				BO2	1.643	0.953	
Na1	8	5	NaO_5	NBO	2.290	0.242	0.967
				NBO	2.338	0.216	
				NBO	2.373	0.199	
				BO2	2.386	0.193	
				NBO	2.600	0.116	
BO1	4	2	OSi_2	Si1 × 2	1.609	1.040	2.080
BO2	8	3	OSi_2Na_1	Si1	1.638	0.965	2.111
				Si1	1.643	0.953	
				Na1	2.386	0.193	
				NBO	2.600	0.116	
NBO	8	5	OSi_1Na_4	Si1	1.578	1.125	1.899
				Na1	2.290	0.242	
				Na1	2.338	0.216	
				Na1	2.373	0.199	
				Na1	2.600	0.116	

^aFor cation origin atoms, M represents O; for oxygen origin atoms, M represents Si and Na, i.e. $n_{\text{O-M}} = n_{\text{O-Si}} + n_{\text{O-Na}}$.

valence of each bond has been calculated using Equation 10. The final column gives the sum of the valences of the bonds to each site, and these sums are close to the formal valence of each origin atom (as required by Equation 11); the valence sums are within $\sim 0.1e$ of the formal valence. Silicon has a valence that is four times larger than that of sodium, and hence the nature of the bonding in the structure is determined primarily by the interaction between silicon and oxygen. For example, for typical bond lengths, Equation 10 shows that a change in valence of 0.05 leads to a small change in Si–O bond length of 0.02 Å, but a much larger change in Na–O bond length of 0.10 Å. Thus the valence sum requirement of Equation 11 is a much stronger constraint on the Si–O bond lengths than it is on the Na–O bond lengths. For the BO1 site, the valence of the two Si–BO bonds is close to one (1.040), as expected. For the BO2 site, there is a reduction in the valence of the Si–BO bonds to ~ 0.96 , so that their total valence is $\sum v_{\text{BO-Si}} = 1.918$; this reduction in Si–BO valence compensates for the additional valence due to the Na–BO bond (0.193), so that the total valence for all bonds to the BO2 site is close to two. Whilst the valence of some Si–BO bonds is reduced to less than one, there is a corresponding increase in the valence of the Si–NBO bond to greater than one (1.125), so that the total valence for all bonds to the Si1 site is close to four. The lengths and valences of the Na–NBO bonds are more widely distributed, but nevertheless their sum is constrained so that the total valence of the Na–BO bonds is close to one. It is interesting to note that the average valence of the Na–NBO bonds, $\bar{v}_{\text{Na-NBO}} = 0.193$, is exactly equal to the valence of the Na–BO bond, so that the Na–BO bond is not weaker than a typical Na–NBO bond.

Explanations of the Na–O bonding in the glass can be provided using essentially the same bond valence description as for the crystal structure. If each NBO in the glass is bonded to four sodium ions, as in the structures of crystals of intermediate composition, then each sodium ion is necessarily bonded to four NBOs (Equation 9). The total Na–O

coordination number is, however, greater than four because there are also some Na–BO bonds. The valence (and hence length) of Na–BO bonds is defined primarily by the Si–BO bonds in the bridge, and the evidence from crystal structures is that there is little variation in this valence. An NBO has only one bond to a silicon atom, and the requirement that the valences of its four Na–NBO bonds plus the valence of the Si–NBO bond add to a total of about two (Equation 11) leaves greater scope for variation in the valences (and lengths) of the individual Na–NBO bonds. Figure 8 shows that the Na–O distribution in the glass is broader than for the crystal structures. The evidence from crystal structures is that the Na–BO distribution is relatively narrow, and furthermore the Na–O coordination is dominated by Na–NBO bonds. Therefore, it may be concluded that the increased width of the Na–O distribution in the glass is associated with the Na–NBO bonds. The BV discussion shows that this broad distribution occurs because the valences of individual Na–NBO bonds are only loosely constrained, even though their sum is more tightly constrained. Clearly the glass has a greater variety of environments for the Na^+ ions than in the crystal, with a broader variation in the lengths of the individual Na–NBO bonds

Figure 8 shows that the Na–O distributions in the crystals are slightly asymmetric, with a sharper leading edge and a broader trailing edge, and the Na–O distribution in the glass has a similar, but more pronounced asymmetry. If the Na–NBO coordination is considered from the point of view of a NBO origin atom, then this asymmetry can be regarded as arising from the exponential form of the bond valence expression (Equation 10). For example, consider a NBO bonded to four Na^+ ions at equal distance d , such that the valences of the four Na–NBO bonds plus the valence of the Si–NBO bond add to a total of two (to satisfy Equation 11). If the length of one of the Na–NBO bonds is shortened to $d - \Delta d$, then its valence is increased by some amount Δv . The valence sum requirement can then be satisfied if a second Na–NBO bond is lengthened so that its valence is reduced by the same amount, $-\Delta v$. However, as a consequence of

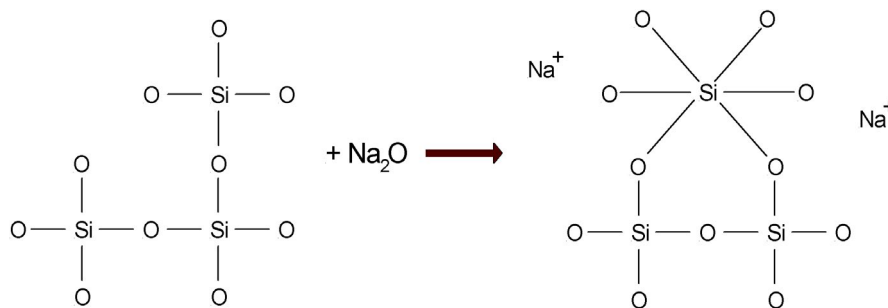


FIGURE 10 Addition of a unit of modifier, such as Na_2O , to a silicate network, resulting in the conversion of one SiO_4 tetrahedron to a SiO_6 octahedron, without the formation of non-bridging oxygens. This mechanism occurs in high pressure phases

the exponential form of Equation 10, this valence reduction leads to a lengthening of the second Na–NBO bond to more than $d+\Delta d$. In this way, the shortening of some Na–NBO bonds leads to a corresponding but greater lengthening of other Na–NBO bonds, resulting in an asymmetric distribution of bond lengths. The asymmetry of the Na–O distribution is akin to the asymmetry of the distribution of Te–O bond lengths in Te–O–Te bridges in tellurites.⁷⁰

The structures of several high pressure sodium silicate crystal phases have been reported,^{71–73} but these have been omitted from the analysis in Figures 5 and 6 and Table 2. In the crystal structures of ambient pressure phases, Na₂O is only incorporated in the silicate network by means of the rupture of Si–O–Si bridges, as shown in Figure 2. However, for high pressure phases, Na₂O may be incorporated by a different mechanism, which involves the formation of a SiO₆ octahedron instead of NBOs, as shown in Figure 10. This is similar to the formation of higher coordinated structural units that arises when modifier is added to borates¹⁴ or germanates.⁷⁴ For HP–Na₂Si₄O₉⁷¹ and HP–Na₂Si₃O₇,⁷² Na₂O is accommodated only by the formation of SiO₆, so that all oxygen atoms are bridging, whilst the formation of both SiO₆ and NBOs occurs in HP–Na₈Si₇O₁₈.⁷³ There are two types of BO in these structures, either between two SiO₄ (a ⁴Si–O–⁴Si bridge), or between a SiO₆ and a SiO₄ (a ⁶Si–O–⁴Si bridge). Oxygens do not occur in a bridge between two SiO₆, because such a site would be severely under-bonded, and triclusters^{75,76} are not found either. These high pressure structures are markedly different to ambient pressure phases, and are not useful for providing structural insight into the sodium environment in ambient pressure glass. For lower soda content (*i.e.* HP–Na₂Si₄O₉⁷¹ and HP–Na₂Si₃O₇⁷²), the coordination shell of sodium is formed entirely of BOs, and is dominated by oxygens in a ⁶Si–O–⁴Si bridge. This is very different to ambient pressure structures in which the coordination shell of sodium is dominated by NBOs, with a smaller contribution from BOs in ⁴Si–O–⁴Si bridges. The bonds from sodium to oxygens in ⁶Si–O–⁴Si bridges tend to be weaker than the Na–O bonds in ambient pressure phases, and the Na–O coordination number is correspondingly larger (typically in the range 7–9) in high pressure phases. For the higher soda phase HP–Na₈Si₇O₁₈,⁷³ there are both SiO₆ and NBOs, and its structural characteristics are intermediate between those of the other high pressure phases and those of the ambient pressure phases.

3.5 | The difference method

The interpretation method described in this paper, in which the (O–O)_{Si} peak is modelled, is a more sophisticated

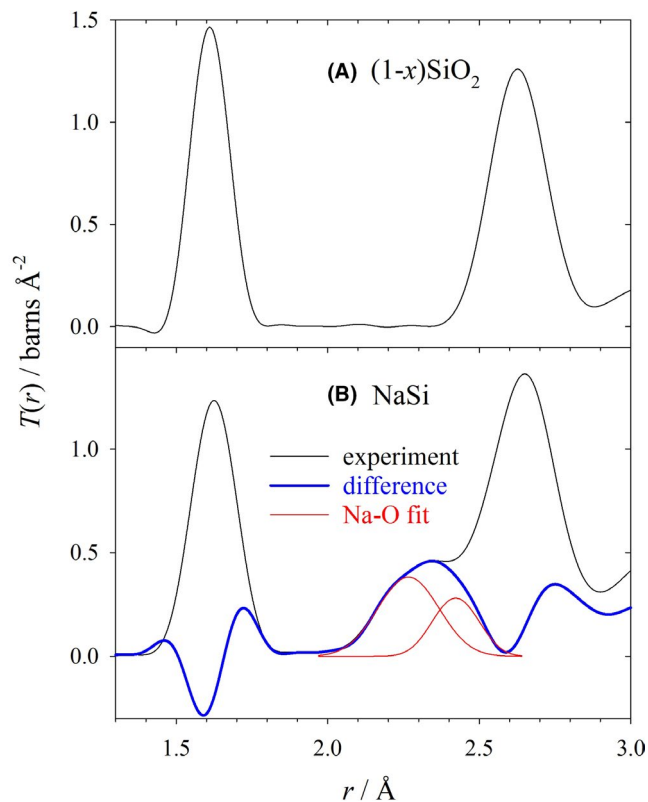


FIGURE 11 Application of the difference method. (A) The total correlation function for pure SiO₂ glass multiplied by a factor $(1-x)$. (B) The total correlation function (black line) for sodium silicate glass with 42.5 mol% Na₂O ($x = 0.425$), the difference, $\Delta T(r)$, according to Equation 16 (thick blue line), and the two components (red lines) of a two-peak fit to the apparent Na–O contribution to the difference

alternative to the traditional analysis technique known as *the difference method*,^{77,78} according to which the correlation function of the network former (e.g., SiO₂) is proportionately subtracted from the correlation function of the modified glass to give that of the network modifier (e.g., Na₂O). For the ND formalism adopted in Section 2.2,¹ in which $T(r)$ is normalized to one average atom, the difference method involves a calculation of

$$\Delta T(r) = T_{\text{NaSi}}(r) - (1-x)T_{\text{SiO}_2}(r), \quad (16)$$

where $T_{\text{SiO}_2}(r)$ and $T_{\text{NaSi}}(r)$ are respectively the correlation functions of pure SiO₂ and of a glass with composition $x\text{Na}_2\text{O} \cdot (1-x)\text{SiO}_2$. (In an alternative ND formalism,⁷⁸ $T(r)$ is defined so that it is normalized to one composition unit, and if the unit is taken to be SiO₂· J Na₂O, where $J = x/(1-x)$, then a direct subtraction of the two correlation functions is required). The two correlation functions used for the difference must be produced in the same way, that is, using the same modification function, with the same value of Q_{max} .

The reason why the Si–O and (O–O)_{Si} peaks can in principle both be removed by the same subtraction is essentially that the numbers of both Si–O and (O–O)_{Si} distances in a SiO₄ tetrahedron are independent of composition.

Figure 11 shows the application of the difference method to the current results. Figure 11A shows $(1 - x) T_{\text{SiO}_2}(r)$, whilst Figure 11B shows $T_{\text{NaSi}}(r)$ for the glass with 42.5 mol% Na₂O (so that $x = 0.425$), both of which were obtained using the Lorch modification function¹ with $Q_{\text{max}} = 43 \text{ \AA}^{-1}$ (see S4 for further details of the measurement for pure SiO₂ glass). Figure 11B also shows the difference, $\Delta T(r)$, obtained according to Equation 16 and a two-peak fit to the apparent Na–O peak (Table S2). Previous ND work^{68–79} has shown the difference method to be inadequate for sodium silicate glasses due to changes in the Si–O and (O–O)_{Si} distances, and the illustration given in Figure 11 shows that changes in the peak widths are also a factor in the failure of the method. The Si–O peak is not removed in $\Delta T(r)$, but instead it leads to a more complex feature at $\sim 1.6 \text{ \AA}$, due to the combined effects of the lengthening and broadening of the Si–O peak on addition of Na₂O to the glass. In the region of the Na–O peak at $\sim 2.3 \text{ \AA}$, $\Delta T(r)$ shows an apparent well-defined peak, after which it returns to a value close to zero. The fit to this apparent Na–O peak yields a total coordination number $n_{\text{Na-O}} = 2.9(2)$, and it corresponds to a total valence sum for a Na⁺ ion of $0.67e$, which is markedly below the ideal value of one. Since the (O–O)_{Si} peak is also expected to lengthen and broaden on addition of Na₂O, this superimposes a similar feature on $\Delta T(r)$ to that observed for the Si–O peak, causing $\Delta T(r)$ to return to zero at $\sim 2.6 \text{ \AA}$. Thus the use of the difference method removes too much weight from the Na–O distribution in this region, resulting in an apparent reduction in average Na–O bond length and coordination. Although Wright, Clare and co-workers have previously attempted to

modify the difference method for sodium silicate glasses,^{68–81} its essential problems were not overcome, and the analysis method presented here is to be preferred.

An inherent assumption of the traditional difference method is that the atom pairs in a structural unit remain the same as the glass composition is altered, with no change in either their separation or number. For more complex glasses, such as borates and germanates for example, in which there is a change in coordination number with composition, it would not be reasonable to even attempt to apply the difference method. As shown in Section 2.1, the oxygen-oxygen coordination numbers can be calculated for more complex glasses, and the analysis method described here can be applied. For example, this approach has already been applied to studies of the environment of lead in lead silicates glasses,^{82,83} sulphate ions in silicate glasses²⁹ and to the structure of lanthanum borogermanate glasses,¹⁵ where the B–B, B–Ge, and La–O peaks were revealed for the first time.

Although sodium silicate is the archetypal example used to illustrate the effect of network modifier on a glass former (e.g., see Figure 2), there are very few reports of experimental determinations of Na–O coordination numbers. In good agreement with the current result of $4.8(2)$, $n_{\text{Na-O}}$ has been reported to be 5.0 in both an EXAFS study of a glass with 33.03 mol% Na₂O⁸⁴ and an EXAFS study of two glasses with 10 and 25 mol% Na₂O.⁸⁵ On the other hand, in the previous ND study $n_{\text{Na-O}}$ was reported as 3.6(9) for a series of five glasses with compositions from 21.8 to 30.8 mol% Na₂O,⁷⁹ but it is likely that this underestimate of the coordination number compared to the current result arises from an underestimate of the width of the (O–O)_{Si} peak (c.f. Figure 4c).

Figure 12 shows the sodium valence sum function,¹⁶ calculated from the measured Na–O distribution according to Equation 12. The long distance limit of this function is 0.88, which is sufficiently close to the ideal value of one (c.f. the valence sums in Table 3) to indicate that the full Na–O coordination may have been identified, although it is also possible that it has been underestimated at longer distances.

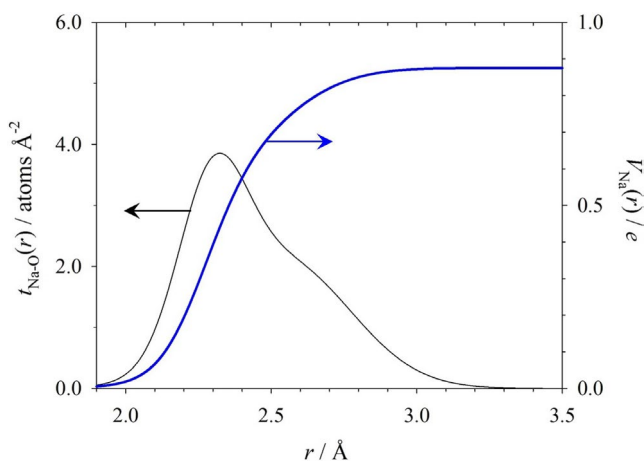


FIGURE 12 Average sodium valence sum function (thick blue line, right hand axis), $V_{\text{Na}}(r)$, calculated from the Na–O partial correlation function (thin black line, left hand axis), $t_{\text{Na-O}}(r)$

4 | CONCLUSIONS

It is shown in this paper that the oxygen-oxygen coordination numbers arising from the structural units in an oxide glass can be calculated, even for glasses that have complex structure or composition. This information is an important basis for simulation of O–O peaks in a neutron correlation function, allowing other correlations at similar distance to be probed in detail, and this is illustrated for a binary sodium silicate glass with 42.50 mol% Na₂O. A survey of sodium silicate crystal structures shows that

the ratio of the mean Si–O and O–O distances in the distorted SiO₄ tetrahedra is virtually the same as the ratio for undistorted tetrahedra. This ratio, together with the predicted (O–O)_{Si} coordination number, allows a fit to be performed to the neutron correlation function, giving an estimate of the distribution of Na–O bond lengths. The fit shows that the total Na–O coordination number for the glass is 4.8(2), at an average Na–O bond length 2.45 Å. The Na–O distribution is found to be asymmetric, with a narrower leading edge, a peak at 2.34 Å, and a broader trailing edge. In sodium silicate crystal structures in this composition range there is a strong preference for sodium to be bonded to four non-bridging oxygens (NBOs), and vice versa. Furthermore, it is found empirically that to a good approximation, the O–Na coordination number is proportional to the molar fraction of Na₂O in the crystal. It is concluded that sodium ions in the glass are bonded predominantly to NBOs and the Na–NBO coordination number may be four as in crystals, with a markedly smaller Na–BO (bridging oxygen) coordination number. Detailed comparison with simulated Na–O distributions for crystals shows that the Na–O distribution in the glass is broader than in crystal structures. Contrary to the conclusions of previous glass structure studies, we do not find evidence that Na–O bonds are shorter for non-bridging oxygens and longer for bridging oxygens. Instead it appears that Na–BO bonds have a narrow distribution, whilst Na–NBO bonds have a broad distribution that extends to both shorter and longer distance than the Na–BO bonds. A bond valence analysis shows that the valence of the bonds to a BO is determined primarily by the two bonded silicon atoms, leaving little scope for variation in the valences and lengths of Na–BO bonds. Contrastingly, a NBO is bonded to only one silicon atom, leaving much greater scope for variation in the valences and lengths of the individual Na–NBO bonds. The asymmetry of the Na–NBO distribution is shown to arise from the exponential form of the bond–valence relationship. The traditional difference method for the analysis of correlation functions derived from diffraction is shown to be unsatisfactory, due to changes with composition of both interatomic distance and width of its distribution.

ACKNOWLEDGEMENTS

Professor Efstratios Kamitsos of the National Hellenic Research Foundation is thanked for illuminating discussions about vibrational spectroscopic investigations of sodium silicate glasses. The authors gratefully acknowledge the Science and Technology Facilities Council (STFC) for access to neutron beam time through allocation nos. RB1320055 and RB1720511 to carry out experiments at the ISIS Pulsed Neutron and Muon Source, U.K.

ORCID

Alex C. Hannon  <https://orcid.org/0000-0001-5914-1295>

Shuchi Vaishnav  <https://orcid.org/0000-0003-4656-0305>

Oliver L. G. Alderman  <https://orcid.org/0000-0002-2342-811X>

[org/0000-0002-2342-811X](https://orcid.org/0000-0002-2342-811X)

Paul A. Bingham  <https://orcid.org/0000-0001-6017-0798>

REFERENCES

- Hannon AC. Neutron diffraction techniques for structural studies of glasses. In: Affatigato M, editor. *Modern glass characterization*. New York: Wiley; 2015. p. 158–240.
- Elliott SR. *Physics of amorphous materials*, 1st edn. Harlow: Longman; 1984.
- Wilkinson CJ, Potter AR, Welch RS, Bragatto C, Zheng Q, Bauchy M, et al. Topological origins of the mixed alkali effect in glass. *J Phys Chem B*. 2019;123:7482–9.
- Bødker MS, Youngman RE, Mauro JC, Smedskjaer MM. Mixed alkali effect in silicate glass structure: viewpoint of ²⁹Si nuclear magnetic resonance and statistical mechanics. *J Phys Chem B*. 2020;124:10292–9.
- Sinclair RN, Wright AC. Neutron scattering from vitreous silica I. The total cross-section. *J Non-Cryst Solids*. 1983;57:447–64.
- Johnson PAV, Wright AC, Sinclair RN. Neutron scattering from vitreous silica II. Twin-axis diffraction experiments. *J Non-Cryst Solids*. 1983;58:109–30.
- Wright AC, Sinclair RN. Neutron scattering from vitreous silica III. Elastic diffraction. *J Non-Cryst Solids*. 1985;76:351–68.
- Grimley DI, Wright AC, Sinclair RN. Neutron scattering from vitreous silica IV. Time-of-flight diffraction. *J Non-Cryst Solids*. 1990;119:49–64.
- Tischendorf B, Ma C, Hammersten E, Venhuizen P, Peters M, Affatigato M, et al. The density of alkali silicate glasses over wide compositional ranges. *J Non-Cryst Solids*. 1998;239:197–202.
- Doweidar H, Feller S, Affatigato M, Tischendorf B, Ma C, Hammarsten E. Density and molar volume of extremely modified alkali silicate glasses. *Phys Chem Glasses*. 1999;40:339–44.
- Barrow N, Packard M, Vaishnav S, Wilding MC, Bingham PA, Hannon AC, et al. MAS-NMR studies of carbonate retention in a very wide range of Na₂O–SiO₂ glasses. *J Non-Cryst Solids*. 2020;534:119958.
- Jellison GE Jr, Feller SA, Bray PJ. A re-examination of the fraction of 4-coordinated boron atoms in the lithium borate glass system. *Phys Chem Glasses*. 1978;19:52–3.
- Hannon AC, Grimley DI, Hulme RA, Wright AC, Sinclair RN. Boroxol groups in vitreous boron oxide: new evidence from neutron diffraction and inelastic neutron scattering studies. *J Non-Cryst Solids*. 1994;177:299–316.
- Hannon AC, Holland D. A parameterisation for the composition-dependence of N₄ in binary borate glasses. *Phys Chem Glasses Eur J Glass Sci Technol B*. 2006;47:449–54.
- Paterson AL, Hannon AC, Werner-Zwanziger U, Zwanziger JW. Structural differences between the glass and crystal phases of LaBGeO₅: neutron diffraction and NMR spectroscopy. *J Phys Chem C*. 2018;122:20963–80.
- Hannon AC. Bonding and structure in network glasses. *J Non-Cryst Solids*. 2016;451:56–67.

17. Hannon AC, Parker JM. The use of bond-valence parameters in interpreting glass diffraction results. *Phys Chem Glasses*. 2002;43C:6–12.
18. Brown ID. *The chemical bond in inorganic chemistry. The bond valence model*, 1st edn. Oxford: Oxford University Press; 2002.
19. Brown ID. Recent developments in the methods and applications of the bond valence model. *Chem Rev*. 2009;109:6858–919.
20. Brown ID, Altermatt D. Bond-valence parameters obtained from a systematic analysis of the Inorganic Crystal Structure Database. *Acta Cryst B*. 1985;41:244–7.
21. Brese NE, O’Keeffe M. Bond-valence parameters for solids. *Acta Cryst B*. 1991;47:192–7.
22. Adams S. Relationship between bond valence and bond softness of alkali halides and chalcogenides. *Acta Cryst B*. 2001;57:278–87.
23. Gagné OC, Hawthorne FC. Comprehensive derivation of bond-valence parameters for ion pairs involving oxygen. *Acta Cryst B*. 2015;71:562–78.
24. Pauling L. *The nature of the chemical bond*, 3rd edn. Ithaca: Cornell University Press; 1960.
25. Allmann R. Beziehungen zwischen Bindungslängen und Bindungsstärken in Oxidstrukturen. *Monatsh Chem*. 1975;106:779–93.
26. Brown ID. Chemical and steric constraints in inorganic solids. *Acta Cryst B*. 1992;48:553–72.
27. Urusov VS. Theoretical analysis and empirical manifestation of the distortion theorem. *Z Kristallogr*. 2003;218:709.
28. Gagné OC, Hawthorne FC. Bond-length distributions for ions bonded to oxygen: alkali and alkaline-earth metals. *Acta Cryst B*. 2016;72:602–25.
29. Vaishnav S, Hannon AC, Barney ER, Bingham PA. Neutron diffraction and Raman studies of the incorporation of sulfate in silicate glasses. *J Phys Chem C*. 2020;124:5409–24.
30. Hannon AC. Results on disordered materials from the General Materials diffractometer, GEM, at ISIS. *Nucl Instrum Meth A*. 2005;551:88–107.
31. Hannon AC. PFIT correlation function fitting software. <http://www.alexhannon.co.uk/>.
32. McDonald WS, Cruickshank DWJ. A reinvestigation of the structure of sodium metasilicate, Na_2SiO_3 . *Acta Cryst*. 1967;22:37–43.
33. Williamson J, Glasser FP. Crystallisation of $\text{Na}_2\text{O}\cdot 2\text{SiO}_2\text{-SiO}_2$ glasses. *Phys Chem Glasses*. 1966;7:127–+.
34. Wright AF, Lehmann MS. The structure of quartz at 25 and 590°C determined by neutron diffraction. *J Solid State Chem*. 1981;36:371–80.
35. Kahlenberg V, Marler B, Muñoz Acevedo JC, Patarin J. Ab initio crystal structure determination of $\text{Na}_2\text{Si}_3\text{O}_7$ from conventional powder diffraction data. *Solid State Sci*. 2002;4:1285–92.
36. Krüger H, Kahlenberg V, Kaindl R. Structural studies on $\text{Na}_6\text{Si}_8\text{O}_{19}$ —a monophyllosilicate with a new type of layered silicate anion. *Solid State Sci*. 2005;7:1390–6.
37. Pant AK, Cruickshank DWJ. The crystal structure of $\alpha\text{-Na}_2\text{Si}_2\text{O}_5$. *Acta Cryst B*. 1968;24:13–9.
38. Pant AK. A reconsideration of the crystal structure of $\beta\text{-Na}_2\text{Si}_2\text{O}_5$. *Acta Cryst B*. 1968;24:1077–83.
39. Kahlenberg V, Langreiter T, Arroyabe E. $\text{Na}_6\text{Si}_2\text{O}_7$ —The missing structural link among alkali pyrosilicates. *Z Anorg Allg Chem*. 2010;636:1974–9.
40. Baur WH, Halwax E, Völlenkle H. Comparison of the crystal structures of sodium orthosilicate, Na_4SiO_4 , and sodium orthogermanate Na_4GeO_4 . *Monatsh Chem*. 1986;117:793–7.
41. McAdam A, Jost KH, Beagley B. Refinement of the structure of sodium Kurrol salt (NaPO_3)_x type A. *Acta Cryst B*. 1968;24:1621–2.
42. Robinson K, Gibbs GV, Ribbe PH. Quadratic elongation—quantitative measure of distortion in coordination polyhedra. *Science*. 1971;172:567–70.
43. Maekawa H, Maekawa T, Kawamura K, Yokokawa T. The structural groups of alkali silicate glasses determined from ^{29}Si MAS-NMR. *J Non-Cryst Solids*. 1991;127:53–64.
44. Stebbins JF. Anionic speciation in sodium and potassium silicate glasses near the metasilicate ($(\text{Na}, \text{K})_2\text{SiO}_3$) composition: ^{29}Si , ^{17}O , and ^{23}Na MAS NMR. *J Non-Cryst Solids*. X. 2020;6:100049.
45. Hannon AC. Neutron diffraction database, <http://www.alexhannon.co.uk/>.
46. Warren BE, Biscoe J. Fourier analysis of X-ray patterns of soda-silica glass. *J Am Ceram Soc*. 1938;21:259–65.
47. Nesbitt HW, Henderson GS, Bancroft GM, Ho R. Experimental evidence for Na coordination to bridging oxygen in Na-silicate glasses: implications for spectroscopic studies and for the modified random network model. *J Non-Cryst Solids*. 2015;409:139–48.
48. Du J, Cormack AN. The medium range structure of sodium silicate glasses: a molecular dynamics simulation. *J Non-Cryst Solids*. 2004;349:66–79.
49. Mountjoy G. The local atomic environment of oxygen in silicate glasses from molecular dynamics. *J Non-Cryst Solids*. 2007;353:1849–53.
50. Soules TF. Molecular dynamic calculation of the structure of sodium-silicate glasses. *J Chem Phys*. 1979;71:4570–8.
51. Newell RG, Feuston BP, Garofalini SH. The structure of sodium trisilicate glass via molecular dynamics employing three-body potentials. *J Mater Res*. 1989;4:434–9.
52. Huang C, Cormack AN. The structure of sodium silicate glass. *J Chem Phys*. 1990;93:8180–6.
53. Huang C, Cormack AN. Structural differences and phase separation in alkali silicate glasses. *J Chem Phys*. 1991;95:3634–42.
54. Cormack AN, Cao Y. Molecular dynamics simulation of silicate glasses. *Molecular Engineering*. 1996;6:183–227.
55. Meyer A, Horbach J, Kob W, Kargl F, Schober H. Channel formation and intermediate range order in sodium silicate melts and glasses. *Phys Rev Lett*. 2004;93:4.
56. Tilocca A, de Leeuw NH. Structural and electronic properties of modified sodium and soda-lime silicate glasses by Car-Parrinello molecular dynamics. *J Mater Chem*. 2006;16:1950–5.
57. Pota M, Pedone A, Malavasi G, Durante C, Cocchi M, Menziani MC. Molecular dynamics simulations of sodium silicate glasses: optimization and limits of the computational procedure. *Comput Mater Sci*. 2010;47:739–51.
58. Machacek J, Gedeon O, Liska M. The MD study of mixed alkali effect in alkali silicate glasses. *Phys Chem Glasses Eur J Glass Sci Technol B*. 2010;51:65–8.
59. Johnson JA, Benmore CJ, Holland D, Du J, Beuneu B, Mekki A. Influence of rare-earth ions on $\text{SiO}_2\text{-Na}_2\text{O-RE}_2\text{O}_3$ glass structure. *J Phys Condens Matter*. 2011;23:065404.

60. Jabraoui H, Vaills Y, Hasnaoui A, Badawi M, Ouaskit S. Effect of sodium oxide modifier on structural and elastic properties of silicate glass. *J Phys Chem B*. 2016;120:13193–205.
61. Li X, Song WY, Yang K, Krishnan NMA, Wang B, Smedskjaer MM, et al. Cooling rate effects in sodium silicate glasses: bridging the gap between molecular dynamics simulations and experiments. *J Chem Phys*. 2017;147.
62. Yu Y, Wang B, Wang M, Sant G, Bauchy M. Reactive molecular dynamics simulations of sodium silicate glasses—toward an improved understanding of the structure. *Int J Appl Glass Sci*. 2017;8:276–84.
63. Deng L, Urata S, Takimoto Y, Miyajima T, Hahn SH, van Duin ACT, et al. Structural features of sodium silicate glasses from reactive force field-based molecular dynamics simulations. *J Am Ceram Soc*. 2020;103:1600–14.
64. Zhou Q, Du T, Guo LJ, Smedskjaer MM, Bauchy M. New insights into the structure of sodium silicate glasses by force-enhanced atomic refinement. *J Non-Cryst Solids*. 2020;536.
65. Kapoutsis JA, Kamitsos EI, Chryssikos GD, Yiannopoulos YD, Patsis AP. Alkali sites in silicate glasses. *Chim Chron, New Ser*. 1994;23:341–6.
66. Hannon AC. XTAL: a program for calculating interatomic distances and coordination numbers for model structures. Rutherford appleton laboratory report RAL-93-063. Rutherford Appleton Laboratory; 1993.
67. Hannon AC. XTAL structural modelling software. <http://www.alexhannon.co.uk/>.
68. Clare AG, Wright AC, Sinclair RN. A comparison of the structural role of Na⁺ network modifying cations in sodium silicate and sodium fluoroberyllate glasses. *J Non-Cryst Solids*. 1997;213:321–4.
69. Wilding M, Badyal Y, Navrotsky A. The local environment of trivalent lanthanide ions in sodium silicate glasses: a neutron diffraction study using isotopic substitution. *J Non-Cryst Solids*. 2007;353:4792–800.
70. Barney ER, Hannon AC, Holland D. Short range order and dynamics in crystalline α -TeO₂. *J Phys Chem C*. 2012;116:3707–18.
71. Fleet ME. Sodium tetrasilicate: a complex high-pressure framework silicate (Na₆Si₃Si₉O₂₇). *Am Miner*. 1996;81:1105–10.
72. Fleet ME, Henderson GS. Sodium trisilicate: a new high-pressure silicate structure (Na₂Si[Si₂O₇]). *Phys Chem Min*. 1995;22:383–6.
73. Fleet ME. Sodium heptasilicate: a high-pressure silicate with six-membered rings of tetrahedra interconnected by SiO₆ octahedra: (Na₈SiSi₆O₁₈). *Am Miner*. 1998;83:618–24.
74. Hannon AC, Di Martino D, Santos LF, Almeida RM. Ge-O coordination in cesium germanate glasses. *J Phys Chem B*. 2007;111:3342–54.
75. Lacy ED. Aluminium in glasses and in melts. *Phys Chem Glasses*. 1963;4:234–8.
76. Macdowell JF, Beall GH. Immiscibility and crystallization in Al₂O₃–SiO₂ glasses. *J Am Ceram Soc*. 1969;52:17–25.
77. Lukesh JS. The distribution of metallic atoms in two-component glasses. *Proc Natl Acad Sci USA*. 1942;28:277–81.
78. Wright AC. The structure of amorphous solids by x-ray and neutron diffraction. *Adv Struc Res Diffraction*. 1974;5:1–120.
79. Wright AC, Clare AG, Bachra B, Sinclair RN, Hannon AC, Vessal B. Neutron diffraction studies of silicate glasses. *Trans Am Cryst Assoc*. 1991;27:239–53.
80. Wright AC, Clare AG, Bachra B, Hannon AC, Sinclair RN, Vessal B. A neutron diffraction study of the structure of alkali silicate glasses. *Bol Soc Esp Ceram*. 1992;31-C:3:77–82.
81. Clare AG, Bachra B, Wright AC, Sinclair RN. The structure of sodium silicate glasses by neutron diffraction. In: Pye LD, Lacourse WC, Stevens HJ, editor. *Physics of non-crystalline solids*. London: Taylor & Francis Ltd, 1992; p. 48–52.
82. Alderman OLG. The structure of vitreous binary oxides: silicate, germanate and plumbite networks. PhD. Thesis, University of Warwick, 2013.
83. Alderman OLG, Hannon AC, Holland D, Feller S, Lehr G, Vitale A, et al. Lone-pair distribution and plumbite network formation in high lead silicate glass, 80PbO.20SiO₂. *Phys Chem Chem Phys*. 2013;15:8506–19.
84. Greaves GN, Fontaine A, Lagarde P, Raoux D, Gurman SJ. Local structure of silicate glasses. *Nature*. 1981;293:611–6.
85. Mazzara C, Jupille J, Flank AM, Lagarde P. Stereochemical order around sodium in amorphous silica. *J Phys Chem B*. 2000;104:3438–45.

SUPPORTING INFORMATION

Additional supporting information may be found online in the Supporting Information section.

How to cite this article: Hannon AC, Vaishnav S, Alderman OLG, Bingham PA. The structure of sodium silicate glass from neutron diffraction and modeling of oxygen-oxygen correlations. *J Am Ceram Soc*. 2021;00:1–17. <https://doi.org/10.1111/jace.17993>